Eur. Phys. J. Plus (2024) 139:624
https://doi.org/10.1140/epjp/s13360-024-05424-4

THE EUROPEAN PHYSICAL JOURNAL PLUS

Regular Article

Crystal channeling investigations at medical synchrotron regimes

Roberto Rossi[1,a], **Attilio Andreazza**[4,5], **Matteo Bauce**[2], **Antonio Carbone**[4,5], **Saverio D'Auria**[4,5], **Marco Garattini**[2], **Geoff Hall**[1], **Tommaso Lari**[5], **Alessio Mereghetti**[3], **Mark Pesaresi**[1], **Marco Pullia**[3], **Paolo Valente**[2], **Alessandro Variola**[2], **Riccardo Zanzottera**[4,5], **Walter Scandale**[1,2,b]

[1] Blackett Laboratory, Imperial College, London SW7 2AZ, UK
[2] INFN Sezione di Roma, Piazzale Aldo Moro, 2, 00185 Rome, Italy
[3] CNAO National Center for Oncological Hadrontherapy, Pavia, Italy
[4] Università degli Studi di Milano, Via Celoria, 16, 20133 Milan, Italy
[5] INFN Sezione di Milano, Via Celoria, 16, 20133 Milan, Italy

Received: 17 November 2023 / Accepted: 25 June 2024
© The Author(s) 2024

Abstract An experimental setup to investigate ion channeling in the hundreds MeV/u energy range is described. A short bent crystal, aligned to the incoming beam by an angular actuator, should deflect ions into a single plane pixel detector used to identify channeled and unchanneled particles. In order to enhance the footprint of channeling on the recorded signals, the incoming particle emittance is tailored on the crystalline plane acceptance by means of massive collimators. Numerical simulations of low energy carbon ions are performed with FLUKA to fully understand the measurement conditions demonstrate the feasibility of the test, to be performed in the experimental room of the National Center for Oncological Hadrontherapy accelerator complex in Pavia, Italy.

1 Introduction

Channeling phenomena develop in crystalline materials when charged particles impinge at angles close to the lattice plane direction. A critical angle can be defined for positively charged particles as $\theta_c = (2U_0/pv)^{1/2}$, where p, v are the particle momentum and velocity, respectively, and U_0 is the well depth of the crystal potential averaged along the planes [1]. When the relative impact angle to the crystalline plane direction is smaller than θ_c, a fraction of particles is captured in channeling states and each particle moves along the crystal oscillating between two neighboring planes. It is possible to deflect charged particles in channeling states with bent crystals if the bending radius is larger than the critical value, $R > R_c = pv/eE_m$ [2], where E_m is the maximum strength of the electric field in the planar channel.

Crystal channeling for beam manipulation has been proved in the past decades with an increasing number of particle species and beam energies. In particular, the UA9 collaboration has gained considerable experience with various applications at CERN for hadron beam collimation in the SPS at 270 GeV and in the LHC at 6.5 TeV [3–6], for beam extraction in the SPS at 400 GeV [7–10], and by implementing more complex schemes for new experimental applications [11–13]. For these applications, crystals have a short length ($\mathcal{O}$ (mm)) and bending angles in the 50 μrad to 300 μrad range. Crystal characterization [14–18] and detailed coherent effect investigations [19–23] have been carried out with dedicated experiments. Tests with heavy ion beams, very relevant for our present investigation, were carried out in both circular machines and extraction lines [5, 24, 25]; to date, crystal channeling has been achieved only with ion beams with energies in the GeV/u ÷ TeV/u range. Previous low energy experiments with both positrons (500 MeV [26]) and protons (1 GeV [27]) were in fact above the regime of medical accelerators. These include the study of other effects of interest for crystal application in circular accelerators, such as the inelastic nuclear interaction and Multiple Coulomb Scattering (MCS).

The profound understanding of crystal-particle interactions has driven sophisticate applications in high-energy particle accelerators. Unconventional beam extraction scenarios have been proposed based on 1) crystal-assisted resonant slow extraction or 2) on the direct extraction with a solely bent crystal [28].

The first scheme is well studied and used for standard operation in the Protvino IHEP U-70 accelerator [29], while the second has been studied at the CERN SPS [30–32]. In all cases, channeling efficiency is expected to increase because of the multi-turn effect [28, 32–34] that affects particles not initially channeled, but rather scattered by a small angle. Turn after turn, these particles have "further chances" to be channeled and extracted, when passing again the crystal at larger impact parameters and within the critical angle.

[a] e-mail: roberto.rossi@cern.ch (corresponding author)
[b] e-mail: walter.scandale@cern.ch (corresponding author)

Published online: 17 July 2024

No attempts have been carried out to extend such extraction methods to ions in the hundreds MeV/u energy range, typical of hadrontherapy machines. Adapting to a medical ion synchrotron the scheme proposed in [28] for the SPS or the U-70 is expect to improve the overall extraction performance and to simplify the accelerator layout. However, the required crystals should have larger bending angles ($\mathcal{O}$(mrad)) to provide the deflection required for extraction in a compact ring. Crystals with such features have already been characterized with various beam energies and species at CERN [18]. Extrapolation of their performance to lower operational energies is based on the following considerations. The cited experiments [26, 27], with beam energies close to the range considered, obtained significant results for channeling efficiency. Simulations [35] indicate that a significant survival rate for low energy ions and protons is expected even for relatively thick crystals, with curvatures larger than the required one.

An experimental layout is proposed to observe channeling and characterize crystals with ion beams in the experimental room (XPR) of the CNAO medical accelerator center [36–38] in Pavia, Italy. Results of simulations, performed with FLUKA [39], demonstrate the feasibility of the crystal characterization within the geometrical constraints of the XPR. Symmetrically, the experimental results should provide an additional validation to the simulation model used in FLUKA to describe crystal-particle interactions of hadrontherapy machines energy. An additional goal is to identify bent crystals to eventually assist beam extraction or beam steering from a medical synchrotron to the patient treatment room.

The layout to be installed in the XPR at CNAO is presented in Sect. 2. The simulations assessing the test feasibility are described in Sect. 3. Conclusions and outlooks are discussed in Sect. 4.

2 Experimental layout

Tests at the CNAO experimental room (XPR) [40] aim to achieve the following results: (1) demonstrate feasibility of crystal channeling with low energy ion beams, (2) evaluate its output ratio and finally (3) establish parametric dependence of the results on crystal characteristics.

Considering the limited space available for the experimental setup (i.e., about ≈ 5 m downstream of the most upstream extraction window), a compact layout for differential measurements of crystal channeling is considered and schematically shown in Fig. 1. The measurement setup will be composed by a short double-slit collimator for beam shaping, a crystal alignment system (goniometer) and a silicon pixel detector (screen). The option of installing the layout (all or only parts of it) in a vacuum tank is considered to reduce the beam scattering with the air, as shown in Fig. 1.

Spatial distributions of particles exiting the crystal will be recorded with the silicon pixel detector while varying the crystal orientation. This will allow to measure the number of deflected particles downstream of the crystal and evaluate the crystal single-pass deflection. The target is to achieve an efficiency level of $\approx 10\%$ to $\approx 20\%$, as obtained in [26, 27] and predicted in [35].

At hadrontherapy beam energies $\mathcal{O}$(100 MeV/u), the channeling critical angle is in the order of ≈ 300 μrad. Detailed values are reported in Table 1. To select a beam with the best shape and divergence to observe channeling, a double-sided collimator will be installed immediately downstream of the extraction window with optimized jaw length, gap and material. The upstream collimator will prepare the beam before it is presented to the crystal: It reduces the beam spot as closely as possible to the crystal impact face dimension and reduces the beam divergence within the critical angle for channeling (see Table 1). Preliminary simulations for optimizing the collimator layout have been performed with the FLUKA Monte Carlo code (see Sect. 3).

The crystal alignment and orientation on the beam are crucial for verification of channeling conditions. The main condition for high efficiency crystal deflection is that the incident beam has a divergence smaller than θ_c [41]. The other condition is the precise

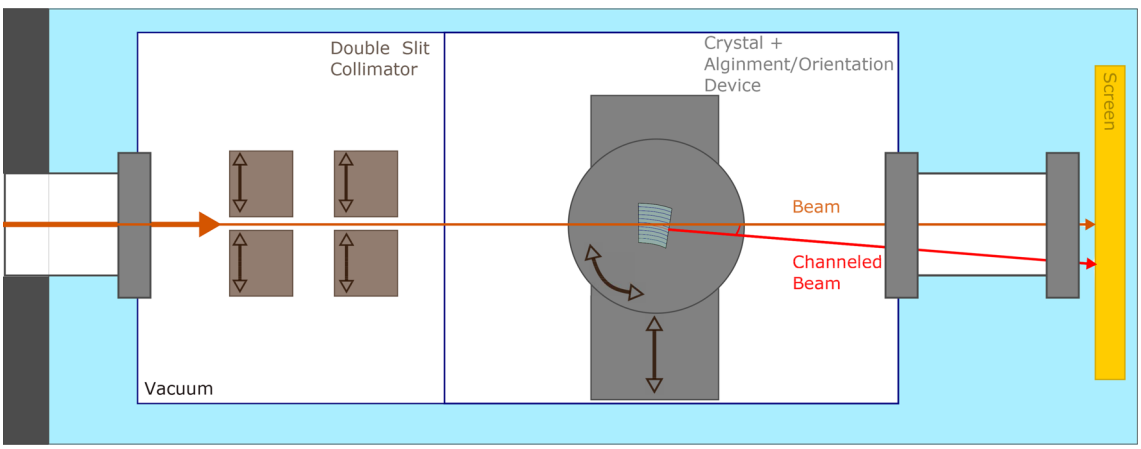

Fig. 1 Proposed experimental layout scheme. Drawings not to scale. The three main components are shown and identified by the labels. In-vacuum regions are depicted in white. The option of performing the experiment in air is considered in the early stages of the test

Table 1 Species and energies foreseen for the initial tests at the CNAO XPR line

For each condition, the critical angle for a silicon crystal is evaluated

Beam species	Energy	Critical angle	Critical radius
$^{12}C^{6+}$	400 MeV/u	223.6 μrad	1.45 mm
$^{12}C^{6+}$	150 MeV/u	365.1 μrad	0.54 mm
p	227 MeV	419.8 μrad	0.42 mm

angular alignment of the crystal to the incoming beam. It is crucial that the goniometer produces well replicable crystal orientations below the critical angle constraint at CNAO beam energies. The angular step of the selected goniometer is ≈ 2 μrad, i.e., considerably smaller than θ_c.

Given the short distance available between the crystal and the detector, a high spatial resolution is required ($\mathcal{O}(10\ \mu m)$) to resolve the different effects that cannot be separated in such small span. The intent is to use both electronics (ITkPix chip) and radiation-hard silicon sensors designed for the ATLAS experiment at the HL-LHC [42, 43].

Two crystals that match the requirements for the experiment are already in use by the UA9 collaboration, which will make them available for the proposed measurement at the CNAO facility. Both crystals can be traversed by the particle beam along two directions (approximately 2 cm and 4 cm long, respectively) and have an adjustable deflection angle up to several mrad. During recent tests with a beam of single charged mixed hadrons at energies of 180 GeV, one of the crystals, set to a deflection of 2.2 mrad, showed a channeling efficiency of $\approx 40\%$ [18]. These crystals will have the principal role of giving information on channeling on a new regime compared to those used in past tests. Long crystals with a large bending angle are at the very edge of what is appropriate at this regime, which is why they are taken into account for the simulation studies presented in Sect. 3.

In addition, other much shorter crystals, $\mathcal{O}(1$ mm) long in the beam direction and with a bending angle of about 1 mrad, are considered for a later phase of the experiment. These characteristics are more suited to the application at hadrontherapy regime.

3 Channeling simulations at hadrontherapy regime

Measurements down to the GeV regime have been performed with shorter crystals and smaller deflection angles, of the order of a few hundred μrad, which still showed efficiencies of 10% to 20% [26, 27]. Moreover, simulations of interaction of carbon ions with bent crystals [35] show a high survival rate even for thicker crystals with larger bending angle.

The FLUKA simulation code has recently been improved [39] to simulate interaction of particles with crystalline lattices; the code has been extensively benchmarked against channeling measurements in various beam regimes. By taking advantage of its capabilities of scaling interactions with the energies and species of beam particles and matter of obstacles, the code has been used to design the experimental layout and to assess the possible channeling efficiency achievable in the experimental conditions. The simulations performed at hadrontherapy regime represent an important test of the predictability power of FLUKA. Two different scenarios are considered in this Section: In the first, the optimization of the experimental setup, in particular the collimator, is investigated; in the second case, having fixed the experimental layout, the channeling experiment was simulated in order to assess its feasibility, understand the experimental signatures and evaluate the effect of the presence of air in the setup.

All the simulations presented in the following paragraphs have been performed with carbon ions at 400 MeV/u. The beam has a Gaussian shape in both horizontal and vertical spatial distribution with $\text{œ}_{\text{beam}}(x, y) = 10$ mm. A Gaussian shape is also considered for the angular distribution with $\text{œ}_{\text{beam}}(x', y') = 1$ mrad.

3.1 Collimator layout optimization

Simulations are used to study the best configuration of the collimator device. The goal is to achieve a design capable of shaping the beam in the transverse spatial and angular distributions, in order to match the emittance to the crystal acceptance in channeling states. The horizontal beam width should not exceed the crystal impact face dimension, in order to maximize the number of beam particles interacting with the crystal and minimize the background hitting the downstream screen sensor. The horizontal beam divergence should not exceed the channeling critical angle for these particles species at the selected operating energies (see Table 1) to maximize the probability of channeling.

The final design foresees two sets of collimator jaws. Each set is separated in the horizontal direction to shape the beam in the same plane as that where beam deflection due to channeling will take place; the gap defines the beam spot size downstream of the collimator. The distance between the two sets of jaws is used to reduce the angular distribution. The results of the preliminary simulations are presented in Fig. 2. To achieve the required specifications, the gap must be ≤ 0.5 mm and the distance close to 1 m.

3.2 Channeling of low energy ions

Once the collimation stage was optimized, FLUKA simulations were performed to predict the channeling interactions in the final experimental layout. The essential characteristics of the simulations are: i. carbon ion beams at 400 MeV/u; Gaussian distribution

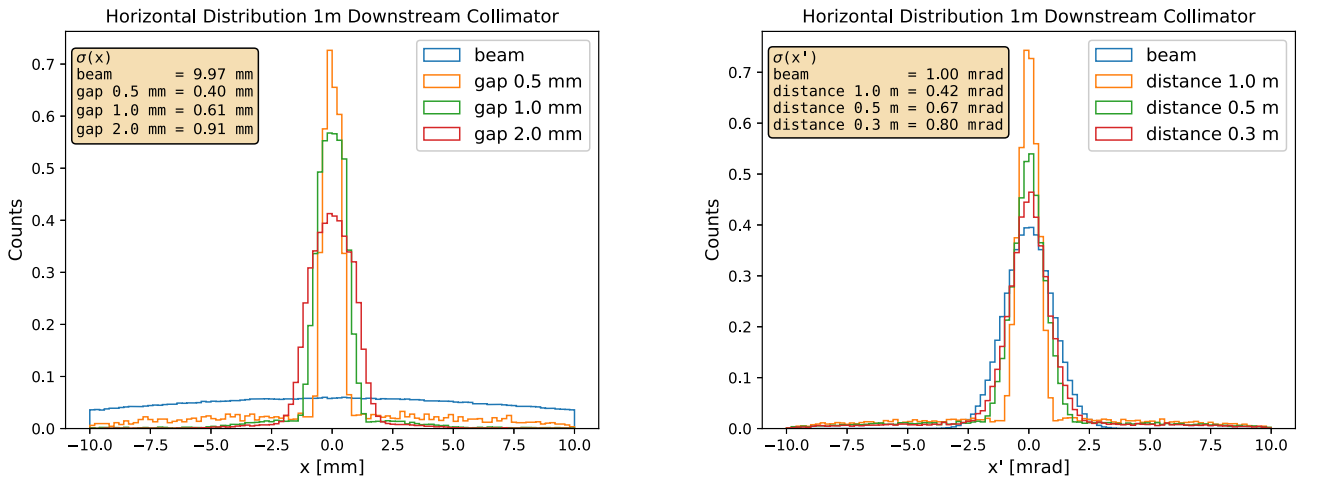

(a) Horizontal spatial distribution 1 m downstream. (b) Horizontal angular distribution 1 m downstream.

Fig. 2 Simulation results obtained with 400 MeV/u carbon ions on the collimator design as sketched in Fig. 1. The different distributions are presented highlighting the effect of the increasing gap between each jaws on the spatial distribution (**a**) and the effect on the angular distribution induced by the reduced distance between the two sets (**b**). In the former case the distance is constant and equal to 1 m, while in the latter it is the gap that is constant at 1 mm. In each figure, the standard deviation of the beam remaining after the collimation stage is reported for every considered scenario; for comparison, the values of the initial the carbon ion beam is given as well

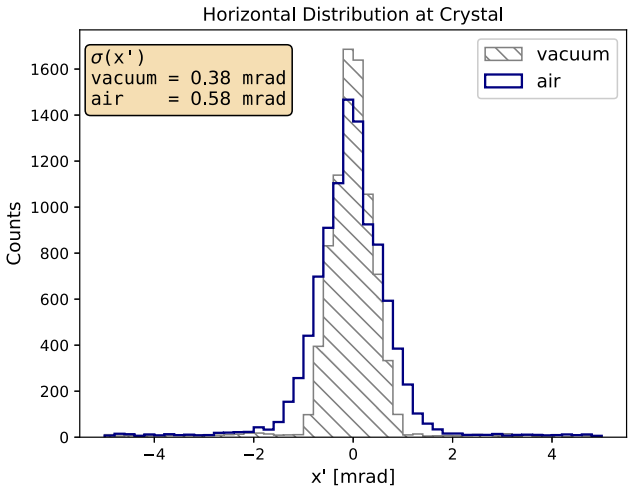

Fig. 3 Beam divergence at the crystal impact face. A beam of $^{12}C^{6+}$ ions with 400 MeV/u energy is shaped by a double set of collimators. Each collimator has a gap between the jaws of 0.5 mm, while the distance between the two sets is of 1 m. With the considered setup in vacuum, the beam divergence impacting the crystal is 0.37 mrad (light blue); while the same setup in air results in a beam divergence of 0.57 mrad (blue), a factor $\sim$ 1.5 larger

with $\text{œ}_{\text{beam}}(x, y) = 10$ mm and $\text{œ}_{\text{beam}}(x', y') = 1$ mrad; ii. the beam is shaped by a two-stages collimator where each jaw is made of tungsten and it is 25 mm long along the beam direction; the gap between each pair of jaws is set to 0.5 mm and the distance between the two sets is 1 m; iii. a crystal with a shorter length and a higher deflection angle to the ones proposed for the measurement is set in channeling just behind the second set of jaws; the crystal is 25 mm long along the beam direction and is set to produce a deflection of 2.2 mrad. The transverse dimension of the crystal impact face is assumed as large as the gap between the collimators jaws, i.e., the full beam emerging from the collimator system interacts with the crystal.

The simulations have been performed with the experimental setup both in vacuum and in air. The effect of air on the beam divergence at the crystal entry face is shown in Fig. 3; while with the setup in vacuum a beam divergence close to θ_c is achieved, this is not the case with the setup in air, for which the angular distribution is increased by about $\sim$50%. Nevertheless, results in air are important since the vacuum tank will be made available at a later stage.

The particle distribution downstream of the crystal is recorded at two positions: 0.5 m and 1.5 m downstream of the second collimator. With FLUKA simulations, the different coherent and incoherent interactions that arise when charged beam particles impinge on a well oriented crystal can be flagged at runtime for a deeper analysis of results. As one can observe from Fig. 4, the onset of channeling (in green) is well separated from the amorphous background 1.5 m downstream of the crystal position, but it is

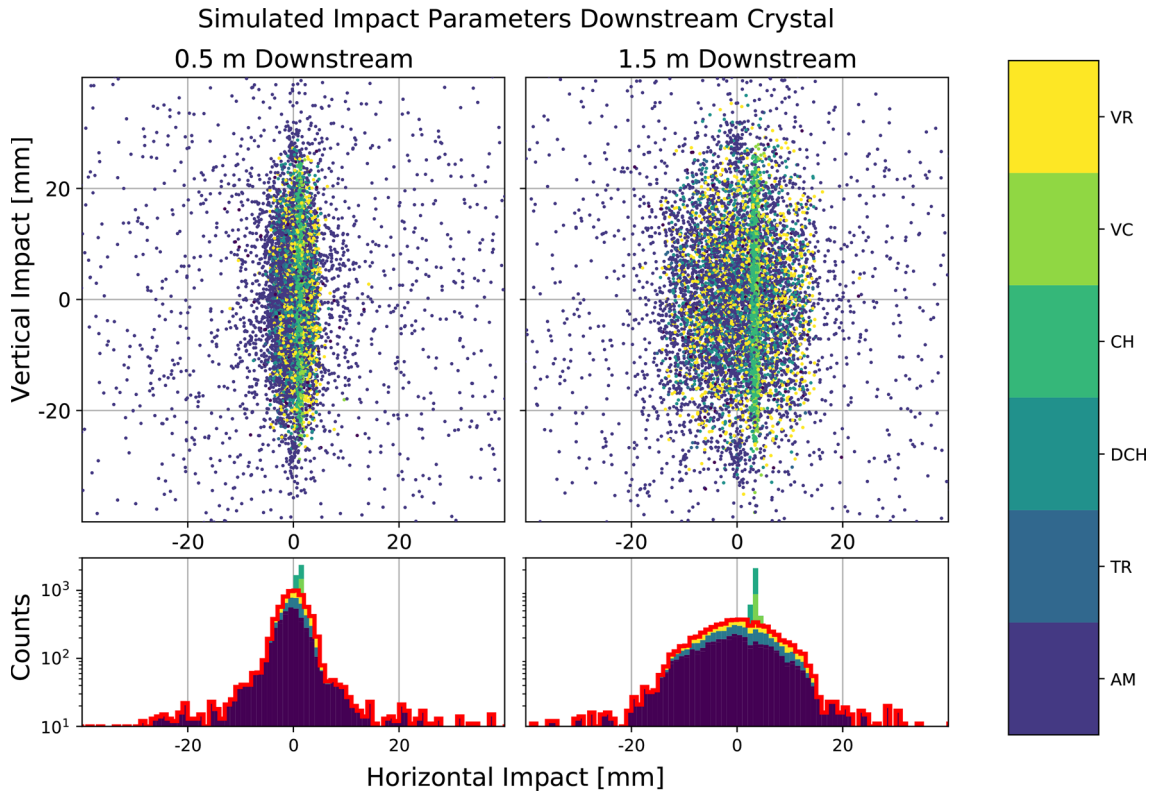

Fig. 4 Simulated particle distributions at two screen locations. The full setup as in Fig. 1 is simulated with FLUKA considering 400 MeV/u $^{12}C^{6+}$ ion beams. Two screens are positioned 0.5 m and 1.5 m downstream of the crystal position. The amorphous distribution that would be generated by a nonoriented crystal is shown by the red solid line. The color code is shown on the bar: amorphous (AM), transition region (TR), dechanneling (DCH), channeling (CH), volume capture (VC) and volume reflection (VR)

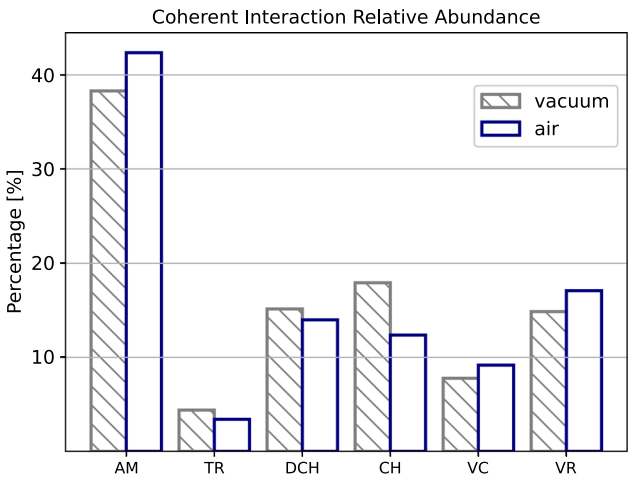

Fig. 5 Relative abundance of coherent and incoherent interactions compared for the simulations with the experimental setup in vacuum (light blue) and in air (blue)

also observable at the closer screen position (i.e., 0.5 m downstream). The excess of particles above the background signal (mainly due to amorphous interactions) is the experimental signature that should be detected as evidence of channeling.

A comparison of the coherent and incoherent effects abundances in the crystal for the layout in vacuum and in air is presented in Fig. 5. The larger beam divergence, that results when the system is in air, reduces the simulated channeling percentage from 17.9 to 12.4%. The opposite trend is observed for both amorphous and dechanneling interactions, the two main sources of background. Both the volume reflection (VR) and the volume capture (VC) represent a larger fraction of the total interactions when the simulation with the experimental setup is in air. This effect is due to the nature of these coherent interactions that arise in the depth of the crystal

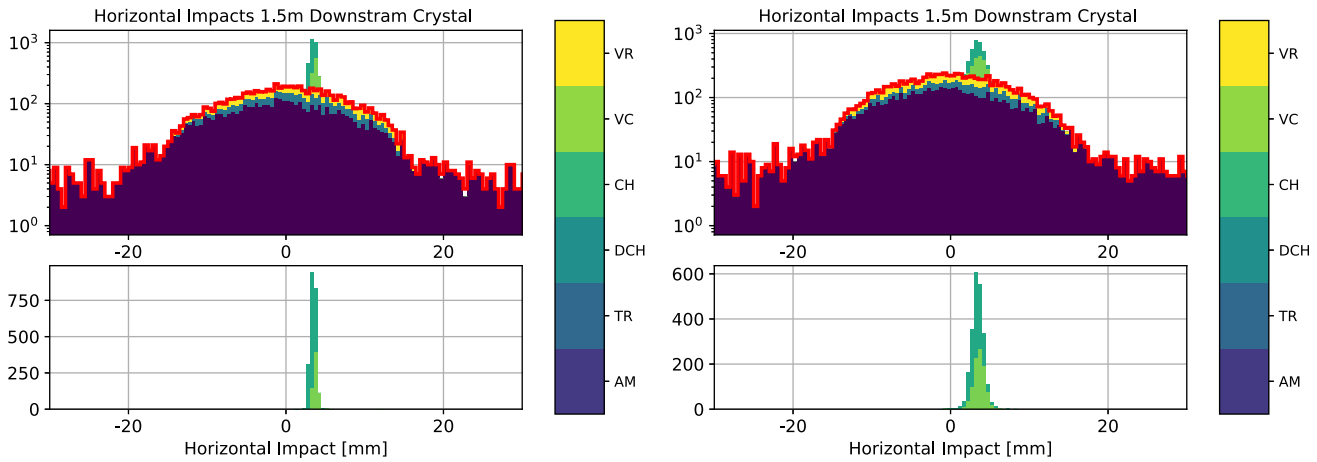

(a) Full simulation layout in vacuum.

(b) Full simulation layout in air.

Fig. 6 Horizontal spatial distribution 1.5 m downstream of the crystal with the experimental setup in vacuum (left frame) and in air (right frame). The same conditions and color code presented in Fig. 4 are used. The bottom plot in both **a** and **b** presents the excess signal with the background (red solid) removed

volume; a larger beam divergence, coupled with the length of the crystal in use, makes the two effects more significant. Indeed, with a shorter crystal the effect of VC and VR would be less important.

As can be observed from Fig. 4, the VC distribution appears at the same position as that of the channeling, with roughly the same standard deviation. Therefore, VC constitutes a background signal that cannot be distinguished in the experimental measurement. However, its relative weight can be estimated by means of simulations and hence correctly taken into account in measurements, for a proper estimation of the fraction of particles that are channeled.

Bearing in mind that the efficiency cannot be directly measured with the proposed experimental layout, it is proposed to compare the experimental results to the simulation using an estimator: the fraction of excess of particles above the background in the region where the channeling is excepted, which will henceforth be referred to as *channeling yield*.

The two FLUKA simulations predict a channeling yield of 17.9% and 12.4 %, again for the system in vacuum and in air, respectively. The methodology is shown in Fig. 6 for both simulations in vacuum (Fig. 6a) and air (Fig. 6b). The background can be removed fitting a Gaussian with a large standard deviation; in these simulations the $\text{œ}_{\text{AM}}(x)$ are 7.7 mm and 7.9 mm for the vacuum and air simulations, respectively. The excess of particles above the background are presented in the bottom plots of Fig. 6. In the simulations, this fraction is estimated to be the 23.1% and 19.2% of the total particles registered on the screen 1.5 m downstream the crystal. Of the particles in the excess above the background, 30.2% and 42.6% come from VC interactions, again for vacuum and air simulations (see Fig. 5). This contribution can be removed to obtain a more accurate estimation of the channeling yield at hadrontherapy regimes.

4 Conclusions and outlook

A design for the experimental measurement of channeling and the estimation of its yield is proposed, exploiting the conditions available in the CNAO experimental room. A double-slit collimation stage has been designed to best establish the beam spatial and angular distribution presented to the crystal. By means of FLUKA simulations, the design is optimized to reduce possible inefficiency sources and match the channeling constraints in this regime. The crystals to carry out a first phase of the tests have already been identified and are made available by UA9. At the same time, the characteristics for new crystals that should be more suitable for the application are identified. The FLUKA simulations have as well provided a deeper understanding of the conditions the measurement will meet. In particular, the VC contribution could have resulted in an overestimation of the channeling yield, had it not been revealed by the simulation. These results are important for the experimental measurement realization.

Once the study on the crystal yield using low energy ions concludes, it will be possible to determine the effect of crystal-assisted extraction performance at medical synchrotrons like that of CNAO. A complete system (consisting of a crystal and its alignment stages) will be developed for both the preliminary experiment on the extracted beam and the hypothetical use in the ring for extraction.

Acknowledgements The authors gratefully acknowledge the UA9 Collaboration that will make available the crystals for our investigation and the DG of the CNAO, who enthusiastically accepted to host the experiment. Imperial College gratefully acknowledges financial support from the UK Science and Technology Facilities Council. INFN sections and Università degli studi di Milano acknowledge the financial support of the MUR (CREMA PRIN No 20227TZ87T).

Data Availability Statement This manuscript has no associated data.

Open Access This article is licensed under a Creative Commons Attribution 4.0 International License, which permits use, sharing, adaptation, distribution and reproduction in any medium or format, as long as you give appropriate credit to the original author(s) and the source, provide a link to the Creative Commons licence, and indicate if changes were made. The images or other third party material in this article are included in the article's Creative Commons licence, unless indicated otherwise in a credit line to the material. If material is not included in the article's Creative Commons licence and your intended use is not permitted by statutory regulation or exceeds the permitted use, you will need to obtain permission directly from the copyright holder. To view a copy of this licence, visit http://creativecommons.org/licenses/by/4.0/.

References

1. J. Lindhard, Influence of crystal lattice on motion of energetic charged particles. Mat. Fys. Medd. Dan. Vid. Selsk **34**, 1–64 (1965)
2. E. Tsyganov, TM-684 (1976)
3. W. Scandale, G. Arduini, R. Assmann, C. Bracco, S. Gilardoni, V. Ippolito, E. Laface, R. Losito, A. Masi, E. Metral et al., Phys. Lett. B **692**(2), 78 (2010)
4. W. Scandale, G. Arduini, M. Butcher, F. Cerutti, M. Garattini, S. Gilardoni, A. Lechner, R. Losito, A. Masi, D. Mirarchi et al., Phys. Lett. B **758**, 129 (2016)
5. R. Rossi, Experimental assessment of crystal collimation at the large hadron collider. Ph.D. thesis, PhD thesis, Universita degli Studi di Roma" La Sapienza (2017)
6. W. Scandale, G. Arduini, R. Assmann, C. Bracco, M. Butcher, F. Cerutti, M. D'Andrea, L. Esposito, M. Garattini, S. Gilardoni et al., Int. J. Mod. Phys. A **37**, 2230004 (2022)
7. L.S. Esposito, P. Bestmann, M. Butcher, M. Calviani, M. Di Castro, M. Donze, M. Fraser, S. Gilardoni, B. Goddard, V. Kain, et al., in *10th International Particle Accelerator Conference (IPAC'19), Melbourne, Australia, 19–24 May 2019* (JACOW Publishing, Geneva, Switzerland, 2019), pp. 2379–2382
8. M. Fraser, R. Alia, B. Balhan, H. Bartosik, J. Bernhard, C. Bertone, D. Björkman, J. Borburgh, M. Brugger, N. Charitonidis, et al., in *10th International Particle Accelerator Conference (IPAC'19), Melbourne, Australia* (2019)
9. F. Velotti, P. Bestmann, M. Butcher, M. Calviani, M. Di Castro, M. Donze, L. Esposito, M. Fraser, S. Gilardoni, B. Goddard, et al., in *10th International Particle Accelerator Conference (IPAC'19), Melbourne, Australia, 19–24 May 2019* (JACOW Publishing, Geneva, Switzerland, 2019), pp. 3399–3403
10. F.M. Velotti, L.S. Esposito, M.A. Fraser, V. Kain, S. Gilardoni, B. Goddard, M. Pari, J. Prieto, R. Rossi, W. Scandale et al., Phys. Rev. Accel. Beams **22**(9), 093502 (2019)
11. C. Barschel, J. Bernhard, A. Bersani, C.B. Meneguolo, R. Bruce, M. Calviani, V. Carassiti, F. Cerutti, P. Chiggiato, G. Ciullo, et al., LHC fixed target experiments: report from the LHC fixed target working group of the CERN physics beyond colliders forum. Ph.D. thesis, CERN Yellow Reports: Monographs Published by CERN (2020)
12. W. Scandale, F. Cerutti, L. Esposito, M. Garattini, S. Gilardoni, S. Montesano, A. Natochii, R. Rossi, G. Smirnov, V. Zhovkovska et al., Nuclear Instrum. Methods Phys. Res. Sect. B **467**, 118 (2020)
13. W. Scandale, G. Arduini, F. Cerutti, M. D'Andrea, L. Esposito, M. Garattini, S. Gilardoni, D. Mirarchi, S. Montesano, A. Natochii et al., Nuclear Instrum. Methods Phys. Res. Sect. A Accel. Spectrom. Detect. Assoc. Equip. **1015**, 165747 (2021)
14. G. Hall, T. James, M. Pesaresi, J. Instrum. **15**(05), C05014 (2020)
15. R. Rossi, G. Cavoto, D. Mirarchi, S. Redaelli, W. Scandale, Nuclear Instrum. Methods **B355**, 369 (2015). https://doi.org/10.1016/j.nimb.2015.03.001
16. W. Scandale, G. Arduini, F. Cerutti, M. Garattini, S. Gilardoni, A. Masi, D. Mirarchi, S. Montesano, S. Petrucci, S. Redaelli et al., Nuclear Instrum. Methods Phys. Res. Sect. B **414**, 104 (2018)
17. W. Scandale, G. Arduini, F. Cerutti, M. Garattini, S. Gilardoni, A. Lechner, R. Losito, A. Masi, D. Mirarchi, S. Montesano et al., Nuclear Instrum. Methods Phys. Res. Sect. B **446**, 15 (2019)
18. R. Rossi, L. Esposito, M. Garattini, T. James, M. Pesaresi, G. Hall, W. Scandale, J. Instrum. **16**(05), P05017 (2021). https://doi.org/10.1088/1748-0221/16/05/p05017
19. W. Scandale, R. Losito, M. Silari, E. Bagli, S. Baricordi, P. Dalpiaz, M. Fiorini, V. Guidi, A. Mazzolari, D. Vincenzi et al., Nuclear Instrum. Methods Phys. Res. Sect. B **268**(17), 2655 (2010)
20. C. Biino, K. Kirsebom, K. Elsener, N.T. Doble, S. Møller, T. Worm, C. Clément, U. Mikkelsen, E. Uggerhøj, L. Gatignon, et al., The influence of radiation damage on the deflection of high-energy beams in bent silicon crystals. Tech. Rep. CERN-SL-96-030-EA (1996). http://cds.cern.ch/record/308375
21. W. Scandale, G. Arduini, F. Cerutti, M. Garattini, S. Gilardoni, A. Lechner, R. Losito, A. Masi, D. Mirarchi, S. Montesano et al., Nuclear Instrum. Methods Phys. Res. Sect. B **438**, 38 (2019)
22. W. Scandale, L. Esposito, M. Garattini, R. Rossi, V. Zhovkovska, A. Natochii, F. Addesa, F. Iacoangeli, F. Galluccio, F. Murtas et al., Eur. Phys. J. C **79**(12), 1 (2019)
23. W. Scandale, F. Cerutti, L. Esposito, M. Garattini, S. Gilardoni, A. Natochii, R. Rossi, G. Smirnov, V. Zhovkovska, F. Galluccio et al., Eur. Phys. J. C **80**(1), 1 (2020)
24. W. Scandale, G. Arduini, R. Assmann, C. Bracco, F. Cerutti, J. Christiansen, S. Gilardoni, E. Laface, R. Losito, A. Masi et al., Phys. Lett. B **703**(5), 547 (2011)
25. S. Redaelli, M. Butcher, C. Barreto, R. Losito, A. Masi, D. Mirarchi, S. Montesano, R. Rossi, W. Scandale, P. Serrano Galvez, G. Valentino, F. Galluccio, Eur. Phys. J. C **81**(2), 1 (2021)
26. S. Bellucci, C. Balasubramanian, A. Grilli, F. Micciulla, A. Raco, A. Popov, V. Baranov, V. Biryukov, Y. Chesnokov, V. Maisheev, Nuclear Instrum. Methods Phys. Res. Sect. B **252**(1), 3 (2006)
27. A. Afonin, V. Baranov, V. Biryukov, M. Breese, V. Chepegin, Y.A. Chesnokov, V. Guidi, Y.M. Ivanov, V. Kotov, G. Martinelli et al., Phys. Rev. Lett. **87**(9), 094802 (2001)
28. W. Scandale, A. Kovalenko, A. Taratin, Nuclear Instrum. Methods Phys. Res. Sect. A Accel. Spectrom. Detect Assoc. Equip. **848**, 166 (2017). https://doi.org/10.1016/j.nima.2016.12.023
29. A. Afonin, V. Baranov, V. Biryukov, V. Chepegin, Y. Chesnokov, Y. Fedotov, A. Kardash, V. Kotov, V. Maisheev, V. Terekhov, E. Troyanov, Nuclear Instrum. Methods Phys. Res. Sect. B Beam Interact. Mater. Atoms **234**(1), 14 (2005). https://doi.org/10.1016/j.nimb.2004.12.128
30. H. Akbari, X. Altuna, S. Bardin, R. Bellazzini, V. Biryukov, A. Brez, M. Bussa, L. Busso, A. Calcaterra, G. Carboni, F. Costantini, R. De Sangro, K. Elsener, F. Ferioli, A. Ferrari, G. Ferri, F. Ferroni, G. Fidecaro, A. Freund, R. Guinand, M. Gyr, W. Herr, A. Hilaire, B. Jensen, J. Klem, L. Lanceri, K. Maier, M. Massai, V. Mertens, S. Møller, S. Morganti, O. Palamara, S. Peraire, S. Petrera, M. Placidi, R. Santacesaria, W. Scandale, R. Schmidt, A.

Taratin, F. Tosello, E. Uggerhøj, B. Vettermann, P. Vita, G. Vuagnin, E. Weisse, S. Weisz, Phys. Lett. B **313**(3), 491 (1993). https://doi.org/10.1016/0370-2693(93)90024-C
31. K. Elsener, G. Fidecaro, M. Gyr, W. Herr, J. Klem, U. Mikkelsen, S. Møller, E. Uggerhøj, G. Vuagnin, E. Weisse, Nuclear Instrum. Methods Phys. Res. Sect. B Beam Interact. Mater. Atoms **119**(1), 215 (1996). https://doi.org/10.1016/0168-583X(96)00239-X
32. X. Altuna, M. Bussa, G. Carboni, B. Dehning, K. Elsener, A. Ferrari, G. Fidecaro, A. Freund, R. Guinand, M. Gyr, W. Herr, J. Klem, M. Laffin, L. Lanceri, U. Mikkelsen, S. Møller, W. Scandale, F. Tosello, E. Uggerhøj, G. Vuagnin, E. Weisse, S. Weisz, Phys. Lett. B **357**(4), 671 (1995). https://doi.org/10.1016/0370-2693(95)00981-P
33. V. Biryukov, Nuclear Instrum. Methods Phys. Res. Sect. B **53**, 202 (1991). https://doi.org/10.1016/0168-583X(91)95659-2
34. A. Taratin, S. Vorobiev, M. Bavizhev, I. Yazynin, Nuclear Instrum. Methods Phys. Res. Sect. B Beam Interact. Mater. Atoms **58**, 103 (1991). https://doi.org/10.1016/0168-583X(91)95683-5
35. C. Ray, D. Dauvergne, Nuclear Instrum. Methods Phys. Res. Sect. B **402**, 313 (2017)
36. S. Rossi, Eur. Phys. J. Plus **126**(8), 78 (2011)
37. S. Rossi, Phys. Med. **31**(4), 333 (2015)
38. M. Pullia, E. Bressi, L. Falbo, A. Garonna, M. Kronberger, T. Kulenkampff, C. Kurfürst, F. Osmić, L. Penescu, M. Pivi, et al., in *7th International Particle Accelerator Conference (IPAC'11), San Sebastián, Spain, September 4–9, 2011* (JACOW, Geneva, Switzerland, 2011), pp. 3589–3591
39. C. Ahdida, D. Bozzato, D. Calzolari, F. Cerutti, N. Charitonidis, A. Cimmino, A. Coronetti, G. D'Alessandro, A. Donadon Servelle, L. Esposito et al., Front. Phys. **9** (2022). https://doi.org/10.3389/fphy.2021.788253
40. M. Pullia, S. Alpegiani, G. Battistoni, J. Bosser, E. Bressi, L. Casalegno, L. Celona, G. Ciavola, M. Ciocca, A. Clozza, et al., in *7th International Particle Accelerator Conference (IPAC'16), Busan, Korea, May 8–13, 2016* (JACOW, Geneva, Switzerland, 2016), pp. 1334–1336
41. W. Scandale, A. Vomiero, S. Baricordi, P. Dalpiaz, M. Fiorini, V. Guidi, A. Mazzolari, R. Milan, G. Della Mea, G. Ambrosi et al., Phys. Lett. B **680**(2), 129 (2009)
42. A. collaboration, et al., CERN, Geneva, Tech. Rep. CERN-LHCC-2017-021. ATLAS-TDR-030 (2017)
43. J. Christiansen, M. Garcia-Sciveres, Extension of RD53 for 3 years to finalize pixel chips for the ATLAS and CMS pixel detector upgrades. Tech. rep. (2021)